Dominance of the particulate organic fraction of soil carbon in the top mineral layer of cold regions

Pablo García-Palacios[1,2]*, Mark A. Bradford[3], Iria Benavente-Ferraces[1], Miguel de Celis[1], Manuel Delgado-Baquerizo[4], Juan Carlos García-Gil[1], Juan J. Gaitán[5,6,7], Asier Goñi-Urtiaga[1], Carsten W. Mueller[8], Marco Panettieri[1], Ana Rey[1], Tadeo Sáez-Sandino[9], Edward A.G. Schuur[10], Noah W. Sokol[11], Leho Tedersoo[12,13], César Plaza[1]

[1]Instituto de Ciencias Agrarias (ICA), CSIC, Serrano 115 bis, 28006, Madrid, Spain
[2]Department of Plant and Microbial Biology, University of Zurich, 8006 Zurich, Switzerland
[3]The Forest School, Yale School of the Environment, Yale University, New Haven, CT 06511, USA
[4]Laboratorio de Biodiversidad y Funcionamiento Ecosistémico. Instituto de Recursos Naturales y Agrobiología de Sevilla (IRNAS), CSIC, Av. Reina Mercedes 10, E-41012, Sevilla, Spain
[5]National Institute of Agricultural Technology (INTA), Institute of Soil Science, Hurlingham, Argentina
[6]National University of Luján, Department of Technology, Luján, Argentina
[7]National Research Council of Argentina (CONICET), Buenos Aires, Argentina
[8]Department of Geosciences and Natural Resource Management, University of Copenhagen, Øster Voldgade 10, DK-1350, Copenhagen K, Denmark
[9]Departamento de Sistemas Físicos, Químicos y Naturales, Universidad Pablo de Olavide; 41013 8 Sevilla, Spain
[10]Center for Ecosystem Society and Science, Northern Arizona University, Flagstaff, AZ, USA
[11]Physical and Life Sciences Directorate, Lawrence Livermore National Laboratory, Livermore, California, USA
[12]Mycology and Microbiology Center, University of Tartu, Tartu, Estonia.
[13]College of Science, King Saud University, Riyadh, Saudi Arabia

*Author for correspondence: Pablo García-Palacios. E-mail: pablo.garcia@ica.csic.es

Abstract

The largest stocks of soil organic carbon (SOC) can be found in cold regions such as arctic, subarctic and alpine biomes, which are warming faster than the global average. Discriminating between particulate and mineral-associated organic carbon (POC and MAOC) can constrain the uncertainty of projected changes in global SOC stocks. Yet MAOC and POC are not considered when assessing the contribution of cold regions to land C-climate feedbacks. Here we synthesize field paired observations of POC and MAOC in the mineral layer, along with experimental warming data, to investigate whether the POC fraction dominates in cold regions and whether this relates to higher SOC losses with warming than in other (milder) biomes. We show that SOC in the first 30 cm of mineral soil is dominated or co-dominated by POC in both permafrost and non-permafrost soils, and in arctic and alpine ecosystems but not in subarctic environments. Our findings indicate that SOC is most vulnerable to warming in cold regions compared to milder biomes, with this vulnerability mediated by higher warming-induced POC losses. The massive accumulation of SOC in cold regions appears predominantly distributed in the more vulnerable POC fraction rather than the more persistent MAOC fraction, supporting the likelihood of a strong, positive land-C climate feedback.

Introduction

Soil organic carbon (SOC) accumulates in cold regions such as arctic, subarctic and alpine environments[1]. Approximately 37% of the global SOC stock, down to a depth of two meters, is stored in these cold regions[2,3], and this vast SOC store is increasingly at risk under climate warming because of the alleviation of temperature limitation for microbial decay[4,5]. Furthermore, the large SOC stocks in cold regions are not only inherently more temperature-sensitive than those in warmer environments[6,7], but will also be subjected to two to four times higher warming rates than the global average due to the Arctic amplification phenomenon[8,9]. Together, these factors set the scene for a dramatic release of C to the atmosphere from SOC stocks in cold regions that will feedback and accelerate anthropogenic global climate warming within a timescale of decades to centuries[3,4].

Different fractions of SOC, that are found within the soil depending on the decomposition pathway of incoming organic matter combined with pedogenic processes, may not respond to global warming in a similar manner[10,11]. For instance, particulate organic C (POC) may be more susceptible to warming-induced microbial decomposition than mineral-associated organic C (MAOC), since POC is not occluded in micropores or microaggregates and/or bound to mineral surfaces, all of which limit microbial accessibility to the organic C in the MAOC fraction[12–14]. Despite the importance of SOC in cold regions for the land C-climate feedback[4,15], no global studies have investigated the dominance of different SOC fractions in these areas. An effort to compare POC versus MAOC proportions in cold ecosystems, mirroring those conducted for tropical and temperate biomes[11,16], will inform whether the fraction composition of SOC points towards a reinforcing or limiting of the land C feedback to climate change from these regions.

A number of features may determine the dominance of POC versus MAOC in cold regions, influencing the mechanisms that control SOC persistence and turnover. In permafrost soils, the perennially frozen ground that remains below 0ºC for at least two consecutive years[17], extremely low temperatures, freeze-thaw dynamics, and water availability and saturated soils are major controls of SOC dynamics[4] and fraction dominance[18,19] compared with non-permafrost soils. Carbon distribution in POC and MAOC can also differ across arctic, subarctic and alpine biomes, as a range of plant and microbial traits, climatic conditions and soil mineralogy play contrasting roles as controls on fraction C concentrations across biome types[11,16,20]. Soil depth may also be important, as the effects of surface cryoturbation in thermokarst-impacted landscapes can increase C association with reactive iron minerals[18,21], forming MAOC over POC. Despite these known process differences, the distribution of SOC across different fractions, biomes, permafrost and non-permafrost soils, and soil depths remains elusive.

We assessed the distribution of SOC in POC and MAOC fractions in the mineral layer of cold regions located in the Northern Hemisphere. Our global literature survey included 134 (the first 30 cm of mineral soil) and 28 (> 30 cm depth) paired POC and MAOC observations from arctic (57), subarctic (41) and alpine (64) biomes (Extended Data Fig. 1). We first addressed whether C in cold regions is predominantly stored in the POC or the MAOC fractions, and whether this dominance changes across soil depths, permafrost and non-permafrost soils, and biome types. Then, we evaluated potential environmental controls (climate, soil properties, active layer thickness, and net primary productivity) on the C stored in the POC versus MAOC fractions. Lastly, we collected data from field sites which experimentally manipulated ambient temperatures, and tested whether climate warming primarily drives SOC losses via changes in the POC or the

MAOC fractions in cold regions (18 observations) compared with other (milder) biomes (22 observations). If C in the top mineral layer is predominantly stored as POC, likely triggering higher relative SOC losses with warming compared to milder biomes, then such a result would build evidence for a potentially dramatic land-C climate feedback involving Earth's cold region soils.

Results

POC dominates or co-dominates in the top mineral layer and across permafrost and biomes

Overall, we found that SOC concentrations in the POC fraction (median: 19.7 g C kg^{-1}, interquartile range (IQR): 38.5) were 40% higher than in the MAOC fraction (median: 14.1 g C kg^{-1}, IQR: 18.7; Fig. 1a). This pattern was confirmed when controlling for multiple environmental drivers by linear mixed-effects (LME) modelling (Extended Data Fig. 2). The dominance of POC over MAOC was most evident when considering only the observations using the particle size fractionation method, but POC still co-dominated with MAOC when using density methods (Extended Data Fig. 3). The higher abundance of POC over MAOC was restricted to the first 30 cm of mineral soil; there was no difference between POC and MAOC in the >30 cm layer (Fig. 1b, Extended Data Fig. 2). The larger concentration of POC relative to MAOC in the first 30 cm of mineral soil was of greater magnitude in permafrost-affected soils than in non-permafrost soils (Fig. 1c, Extended Data Fig. 2), with 75% and 68% increases in the corresponding medians, respectively. At the biome level, POC was significantly greater than MAOC concentration in the first 30 cm of mineral soil in arctic and alpine sites, but not in the subarctic sites (Fig. 1d). Both fractions increased with SOC (Fig. 2), but the slope was steeper for POC (slope: 0.66, $P < 0.001$) than for MAOC (slope: 0.34, $P < 0.001$). As a consequence, POC became more dominant relative to MAOC as SOC concentration increased.

POC and MAOC in the top mineral layer are not associated with the same environmental drivers

Separate linear-mixed effects models for each C fraction (Fig. 3) indicated that POC and MAOC were negatively associated with MAT (estimate: -0.29, 95% confidence interval (CI): -0.84 to 0.29; and estimate: -0.72, 95% CI: -1.20 to -0.24, respectively), but positively with MAP (estimate: 0.49, 95% CI: -0.04 to 0.99; and estimate: 0.75, 95% CI: 0.33 to 1.18, respectively). NPP increased POC (estimate: 0.61, 95% CI: 0.15 to 1.08) but did not affect MAOC. We also found a positive association between both C fractions and soil clay + silt content (estimate: 0.65, 95% CI: 0.22 to 1.11, for POC; and estimate: 0.55, 95% CI: 0.18 to 0.93, for MAOC). To build confidence in our conclusions from this analysis of our observational dataset, we also addressed the relative importance of the environmental drivers using random forests modelling. We found that the most important predictors of POC (NPP and soil clay + silt) and MAOC (MAT and soil clay + silt) in the random forests models (Extended Data Figure 4) were also significant predictors in the linear-mixed effects models (Fig. 3).

SOC in the top mineral layer is more vulnerable to experimental warming in cold systems than in other biomes

There was a tendency for decreased SOC with warming in cold regions (mean percentage change [MPC]: -15.46%; CI: -30.16 to 2.33; Fig. 4, Supplementary Table 1) but not in the other biomes' category (MPC: -0.30%; CI: -13.15 to 14.45). In line with this result, we found a significant negative effect of warming on POC in cold regions (MPC: -27.89%; CI: -47.48 to -0.90) but not in other biomes (MPC: 17.00%; CI: -4.40 to 43.33). The results of the meta-regression confirmed the differential effects of warming on POC in cold regions compared to other biomes, as biome type was a significant moderator (P = 0.008). MAOC did not respond to warming in either cold regions or other biomes.

Discussion

Soils represent the largest actively cycling pool of C in terrestrial ecosystems, holding more C than plants and the atmosphere combined[2,22]. Cold regions such as arctic, subarctic and alpine environments store a massive SOC stock that is being released to the atmosphere under anthropogenic global warming, intensifying climate change[5,15]. The mineral protection of soil organic matter (i.e., the formation of MAOC) has been proposed as a fundamental mechanism controlling the long-term persistence of SOC[10,23]. Our observational analysis demonstrates that SOC in the top mineral layer of cold regions (the first 30 cm of mineral soil) is dominated on average, however, not by MAOC but by the POC fraction, both in permafrost and non-permafrost soils, as well as in arctic and alpine ecosystems (though not in subarctic environments). The synthesis of experimental warming studies suggests that SOC is more vulnerable to warming in cold ecosystems compared to milder biomes, given higher warming-induced POC losses. The large SOC stocks in cold regions are not only subjected to a higher degree of warming than the global average[8], but proportionally more of the SOC is stored in the POC fraction – the fraction most vulnerable to anthropogenic climate warming.

The relationship between soil C inputs and outputs balances the global SOC stock on an annual basis[24]. However, climate warming may destabilize this balance, because microbial-mediated SOC losses under warming are expected to increase more than soil C inputs from plant residues[5]. The net outcome of these warming effects is uncertain in cold regions[25], but the relative dominance we observed of the POC fraction compared to the MAOC fraction may point towards higher SOC losses than expected due to faster C turnover in these cold environments. Such an effect may be particularly conspicuous under high emission scenarios, where gains in vegetation C are not large enough to compensate for SOC losses[26]. In permafrost-affected soils, POC dominates or co-dominates C concentration (Fig. 1c), which may render the total SOC pool more susceptible to rapid microbial breakdown upon permafrost thaw[27,28]. These results are relevant at the global scale, because the permafrost C-climate feedback has been projected to account for 0.27 ºC additional global warming by 2100 and up to 0.42 ºC by 2300 in high emissions scenarios[4,25]. The representation of SOC fractions in biogeochemical models may help to constrain the uncertainty of projected change in global SOC estimates[18], as has been demonstrated in other global biomes[16].

The potential for large SOC losses under warming as a result of high POC concentrations may be modulated because the concentration of MAOC in permafrost soils may shift under climate change. For instance, warming-induced increases in iron-bound organic C have been found upon a permafrost thaw sequence on the Qinghai-Tibet Plateau[18]. Thus, alongside the initial C release from the microbial decomposition of the POC fraction, an increase in the stability of the MAOC fraction may dampen the gradual permafrost C–climate feedback over decades or centuries – i.e. the timescale where these feedbacks are more likely to cause abrupt climate change[4]. In our study we used the increase in the active layer thickness as a surrogate of warming-induced permafrost thaw, which is commonly used in permafrost-carbon feedback modelling[29,30]. Interestingly, the increased thickness of the active layer is associated with a higher relative dominance of MAOC over POC in the total SOC (fMAOC, Pearson's $r = 0.29$, $P = 0.03$, Extended Data Fig. 5). On the other hand, waterlogging and oxygen limitation across a spatial gradient of permafrost thaw have also been found to induce the dissolution of iron minerals and release of MAOC in the arctic permafrost[31]. Therefore, whether changes in the stability of MAOC upon long-term permafrost thaw can alleviate POC losses with warming remains a critical issue to constrain the land C-climate feedback from cold regions. To address this unknown, more direct evaluations of thaw dynamics at sentinel sites may help to overcome the limitations of space for time approaches.

The dominance of POC over MAOC is more evident when considering the size fractionation studies only, which encompass a larger number of observations across a wider biome distribution than density studies (Extended Data Figure 3). However, studies using density methods still reveal co-dominance of POC with MAOC, as opposed to the MAOC dominance expected from work in temperate and tropical biomes[11,13]. Overall, the consideration of both physical fractionation methods in our analysis contributes to a more conservative assessment of POC contributions to total SOC, as performed for other terrestrial ecosystems[11,16,32]. Our quantitative synthesis also demonstrates that whereas SOC in the first 30 cm of mineral soil is largely dominated by the POC fraction, the pattern is not found at deeper soil layers (> 30 cm). The ubiquity of this finding is uncertain because the number of studies including subsoil data was much lower compared to those on topsoils. The assessment of SOC from cold systems at deep soil layers such as in Yedoma deposits remains a priority for soil C research, and we further advocate to include POC and MAOC fractions in such efforts to improve the prediction of SOC vulnerability to climate warming.

Our results further indicate that in arctic and alpine biomes, POC dominates or co-dominates SOC in the top 30 cm of mineral soil. The large accumulations of undecomposed plant residues in the organic horizon and excess soil moisture may be the precursor to the higher POC observed in the arctic and in swamp meadows of the Tibetan plateau[33,34], although other mechanisms may operate in drier alpine steppes. Also, the reactivity of soil minerals is very low under the permafrost conditions in these areas[35], while the portion of undecomposed soil organic matter with reduced functional groups is high, which limits the occurrence of organo-mineral interactions[23]. In contrast to MAOC, C accumulation in the POC fraction is not dependent on a finite availability of mineral surfaces to interact with[20], and can in theory accumulate indefinitely if C inputs are not limiting. Such a dynamic appears consistent with the steeper slope of the SOC vs. POC than the SOC vs. MAOC relationship that was driven by higher POC concentrations at the arctic sites (Fig. 2).

Concentrations of MAOC and POC in cold regions were associated with a set of distinct and overlapping environmental drivers, as confirmed by both linear-mixed and random forest modelling (Fig. 3 and Extended Data Fig. 4). Whereas MAOC was mainly linked with climate and soil clay + silt content, POC was related with plant inputs (NPP) and soil clay + silt content. The MAT emerged as a strong predictor of MAOC concentration, with higher MAOC concentrations at lower temperatures, highlighting the strong role of temperature limitation for persistence of the mineral-protected fraction. Soil clay + silt content positively affected both fractions, indicating that POC and MAOC are higher in clayey soils that host larger mineral surface area and reactive sites for C adsorption[36,37]. However, the lack of data on predictors in the studies included in the meta-analysis prevented us from addressing the contribution of other potentially important soil mineralogical variables for organo-mineral interactions, particularly the mineral type, the proportion of reactive minerals, their specific surface area and the availability of binding sites[16]. There was a positive relationship between POC and NPP, suggesting that, beyond potential effects of the build-up of relatively undecomposed plant material in the organic horizons[18,38], increased plant C inputs likely also contribute to C accumulation in the POC fraction of the mineral layer. We call for future empirical studies addressing a full suite of biological, chemical and mineralogical soil properties to gain mechanistic insights into POC and MAOC distributions in cold regions.

Finally, we found more pronounced SOC and POC losses from the mineral layer with experimental warming in cold regions than in other (milder) biomes (Fig. 4). These results confirmed the pattern found in a previous meta-analysis[39], where POC losses with warming increased with latitude. Climate warming decreases the temperature limitation for microbial decomposition of POC in cold ecosystems[7,40], and this likely drives the greater POC and SOC losses. Conversely, POC increased with warming in other biomes, although this response was not significant. In these milder biomes, warming-induced increases in net primary production are more likely to compensate or even outpace soil respiratory losses[5], which are not as sensitive to temperature as in cold regions[6,7]. However, we caution that we only evaluated warming studies which reported fraction data, which markedly reduced the number of studies available for synthesis. The minimal, mean change in total SOC under experimental warming in other biomes may then not be representative of broader patterns. As such, we suggest that the most valid interpretation of our findings is that SOC losses are likely relatively greater in cold biomes due to the sensitivity of POC decomposition to warming. To gain mechanistic understanding on POC losses with warming in cold regions, future empirical research needs to quantify C inputs from plant growth and C outputs from microbial decomposition, and consider warming effects on the overlying organic horizon. Also, the mechanisms behind POC losses with warming may be different in non-permafrost soils and in soils affected by gradual permafrost thaw, compared to soils suffering from abrupt thaw. In regions experiencing abrupt permafrost thaw, the mineral protection of SOC may be less efficient due to enhanced soil aeration[41] and increased lateral C transport through gullies and slumps in thermokarst-impacted sites[42]. Nevertheless, in the much larger permafrost areas experiencing more gradual thawing, and in non-permafrost soils, the size of POC likely exceeds the capacity of the soil mineral matrix to dampen losses of SOC from microbial decomposition under warming climates. The relative dominance of the POC fraction and its higher vulnerability to increased warming point towards a reinforcing of the land C feedback to climate change from cold regions.

Conclusion

We observed that C in the top mineral layer of cold regions dominates or co-dominates on average in the POC fraction compared to the MAOC fraction. This pattern was found in permafrost-affected sites and also in those sites without a permafrost layer, and in arctic and alpine ecosystems but not in subarctic environments. Concentrations of MAOC and POC were associated with different sets of environmental drivers, with MAOC mainly linked with climate and soil parameters and POC with plant inputs and soil parameters. The dominance of POC agreed with the higher temperature vulnerability of SOC found in cold compared with milder biomes, as mediated by higher warming-induced POC losses in the former. Recent research and international initiatives have profoundly advanced our understanding of the contribution of SOC from cold regions to global climate regulation, from increased microbial breakdown of SOC with warming[7], to the quantification of SOC within deeper soil profiles[34] and the effects of permafrost thaw timing (gradual vs. abrupt)[30]. However, the emerging SOC fraction framework has not yet been integrated into such large spatiotemporal studies. Our study demonstrates the relative dominance of the POC fraction in cold regions, sets a critical baseline for understanding how the massive SOC stock in these areas will respond to climate change, and builds evidence for a dramatic land-C climate feedback driven by Earth's cold biomes.

References

1. Crowther, T. W. *et al.* The global soil community and its influence on biogeochemistry. *Science* **365**, eaav0550 (2019).
2. Jackson, R. B. *et al.* The ecology of soil carbon: pools, vulnerabilities, and biotic and abiotic controls. *Annu. Rev. Ecol. Evol. Syst.* **48**, 419–445 (2017).
3. Schuur, E. A. G. *et al.* Permafrost and climate change: carbon cycle feedbacks from the warming arctic. *Annu. Rev. Environ. Resour.* **47**, 343–371 (2022).
4. Schuur, E. A. G. *et al.* Climate change and the permafrost carbon feedback. *Nature* **520**, 171–179 (2015).
5. García-Palacios, P. *et al.* Evidence for large microbial-mediated losses of soil carbon under anthropogenic warming. *Nat. Rev. Earth Environ.* **2**, 507–517 (2021).
6. Carey, J. C. *et al.* Temperature response of soil respiration largely unaltered with experimental warming. *Proc. Natl. Acad. Sci. U. S. A.* **113**, 13797–13802 (2016).
7. Koven, C. D., Hugelius, G., Lawrence, D. M. & Wieder, W. R. Higher climatological temperature sensitivity of soil carbon in cold than warm climates. *Nat. Clim. Chang.* **7**, 817–822 (2017).
8. Rantanen, M. *et al.* The Arctic has warmed nearly four times faster than the globe since 1979. *Commun. Earth Environ.* **3**, 1–10 (2022).
9. Jansen, E. *et al.* Past perspectives on the present era of abrupt Arctic climate change. *Nat. Clim. Chang.* **10**, 714–721 (2020).
10. Lavallee, J. M., Soong, J. L. & Cotrufo, M. F. Conceptualizing soil organic matter into particulate and mineral-associated forms to address global change in the 21st century. *Glob. Chang. Biol.* **26**, 261–273 (2020).
11. Sokol, N. W. *et al.* Global distribution, formation and fate of mineral-associated soil organic matter under a changing climate: A trait-based perspective. *Funct. Ecol.* **36**, 1411–1429 (2022).
12. Benbi, D. K., Boparai, A. K. & Brar, K. Decomposition of particulate organic matter is more sensitive to temperature than the mineral associated organic matter. *Soil Biol. Biochem.* **70**, 183–192 (2014).

13. Lugato, E., Lavallee, J. M., Haddix, M. L., Panagos, P. & Cotrufo, M. F. Different climate sensitivity of particulate and mineral-associated soil organic matter. *Nat. Geosci.* **14**, 295–300 (2021).

14. Liu, X. J. A. *et al.* Soil aggregate-mediated microbial responses to long-term warming. *Soil Biol. Biochem.* **152**, 108055 (2021).

15. Zimov, S. A., Schuur, E. A. G. & Iii, F. S. C. Permafrost and the global carbon budget. *Science* **312**, 1612–1613 (2006).

16. Georgiou, K. *et al.* Global stocks and capacity of mineral-associated soil organic carbon. *Nat. Commun.* **13**, 1–12 (2022).

17. Schuur, E. A. G. & MacK, M. C. Ecological response to permafrost thaw and consequences for local and global ecosystem services. *Annu. Rev. Ecol. Evol. Syst.* **49**, 279–301 (2018).

18. Liu, F. *et al.* Divergent changes in particulate and mineral-associated organic carbon upon permafrost thaw. *Nat. Commun.* **13**, 1–10 (2022).

19. Gentsch, N. *et al.* Temperature response of permafrost soil carbon is attenuated by mineral protection. *Glob. Chang. Biol.* **24**, 3401–3415 (2018).

20. Cotrufo, M. F., Ranalli, M. G., Haddix, M. L., Six, J. & Lugato, E. Soil carbon storage informed by particulate and mineral-associated organic matter. *Nat. Geosci.* **12**, 989–994 (2019).

21. Joss, H. *et al.* Cryoturbation impacts iron-organic carbon associations along a permafrost soil chronosequence in northern Alaska. *Geoderma* **413**, 115738 (2022).

22. IPCC. Assessment Report 6 Climate Change 2021: The Physical Science Basis. (2021).

23. Lehmann, J. & Kleber, M. The contentious nature of soil organic matter. *Nature* **528**, 60–68 (2015).

24. Davidson, E.A., Janssens, I. A. Temperature sensitivity of soil carbon decomposition and feedbacks to climate change. *Nature* **440**, 165–73 (2006).

25. Burke, E. J. *et al.* Quantifying uncertainties of permafrost carbon-climate feedbacks. *Biogeosciences* **14**, 3051–3066 (2017).

26. McGuire, A. D. *et al.* Dependence of the evolution of carbon dynamics in the northern permafrost region on the trajectory of climate change. *Proc. Natl. Acad. Sci. U. S. A.* **115**, 3882–3887 (2018).

27. Dutta, K., Schuur, E. A. G., Neff, J. C. & Zimov, S. A. Potential carbon release from permafrost soils of Northeastern Siberia. *Glob. Chang. Biol.* **12**, 2336–2351 (2006).

28. Elberling, B. *et al.* Long-term CO2 production following permafrost thaw. *Nat. Clim. Chang.* **3**, 890–894 (2013).

29. Miner, K. R. *et al.* Permafrost carbon emissions in a changing Arctic. *Nat. Rev. Earth Environ.* **3**, 55–67 (2022).

30. Turetsky, M. R. *et al.* Carbon release through abrupt permafrost thaw. *Nat. Geosci.* **13**, 138–143 (2020).

31. Patzner, M. S. *et al.* Iron mineral dissolution releases iron and associated organic carbon during permafrost thaw. *Nat. Commun.* **11**, 1–11 (2020).

32. Prairie, A. M., King, A. E. & Cotrufo, M. F. Restoring particulate and mineral-associated organic carbon through regenerative agriculture. *Proc. Natl. Acad. Sci.* **120**, 2217481120 (2023).

33. Ping, C. L. *et al.* High stocks of soil organic carbon in the North American Arctic region. *Nat. Geosci.* **1**, 615–619 (2008).

34. Mishra, U. *et al.* Spatial heterogeneity and environmental predictors of permafrost region soil organic carbon stocks. *Sci. Adv.* **7**, 1–13 (2021).

35. Ping, C. L., Jastrow, J. D., Jorgenson, M. T., Michaelson, G. J. & Shur, Y. L. Permafrost soils and carbon cycling. *Soil* **1**, 147–171 (2015).

36. Hassink, J. The capacity of soils to preserve organic C and N by their association with clay and silt particles. *Plant Soil* **191**, 77–87 (1997).

37. Cotrufo, M. F. & Lavallee, J. M. Soil organic matter formation, persistence, and functioning: A synthesis of current understanding to inform its conservation and regeneration. *Adv. Agron.* **172**, 1–66 (2022).

38. Prater, I. *et al.* From fibrous plant residues to mineral-associated organic carbon - The fate of organic matter in Arctic permafrost soils. *Biogeosciences* **17**, 3367–3383 (2020).

39. Rocci, K. S., Lavallee, J. M., Stewart, C. E. & Cotrufo, M. F. Soil organic carbon response to global environmental change depends on its distribution between mineral-associated and particulate organic matter: A meta-analysis. *Sci. Total Environ.* **793**, 148569 (2021).

40. Allison, S. D., Wallenstein, M. D. & Bradford, M. A. Soil-carbon response to warming dependent on microbial physiology. *Nat. Geosci.* **3**, 336–340 (2010).

41. Liu, F. *et al.* Altered microbial structure and function after thermokarst formation. *Glob. Chang. Biol.* **27**, 823–835 (2021).

42. Abbott, B. W. *et al.* Biomass offsets little or none of permafrost carbon release from soils, streams, and wildfire: An expert assessment. *Environ. Res. Lett.* **11**, (2016).

Methods

The soil profile in cold regions typically consists of a surface organic horizon (O) overlaying different layers of top and subsoil mineral horizons (A, B and C)[35]. Considering that the mineral horizon contains the largest amount of SOC in cold regions[34,43], with the exception of deep Yedoma sediments[44], and that the organic horizon is exclusively dominated by POC in the form of moderately decomposed plant material[18,38], we restricted our POC vs. MAOC comparison to the mineral layer.

Meta-analysis of the distribution of soil organic carbon fractions in cold systems

We synthesized studies that measured SOC, POC and MAOC concentrations (g C kg soil^{-1}) in the soil mineral layer of terrestrial ecosystems from cold regions (arctic, subarctic and alpine biomes following the Köppen-Geiger climate classification; Extended Data Fig. 1). The organic layer was not included in our study, and thereby soil C data comes exclusively from the mineral layer, independently of the presence or not of the organic layer in the study site. We selected paired observations of POC and MAOC at each site.

A literature search was conducted on 4th May 2022 in the ISI Web of Knowledge with no restriction on publication year using the following term combinations: (soil carbon or soil organic carbon) and (fraction* or POM or MAOM or mineral or particulate or physical protection or light fraction* or macroaggreg* or microaggreg* or occluded or stabiliz* or persisten*) and (boreal or arctic or subarctic or tundra or permafrost or alpine). We screened previous reviews on the topic to check for missing papers[11]. Then, we confronted this list with our selection criteria (see Supplementary Table 2). Data from two unpublished studies meeting the selection criteria were also included in the database, one performed at the CiPERH site in Alaska[45] and one from a global network of terrestrial ecosystems. Studies conducted in Antarctica were removed since soil organic matter formation and turnover are controlled by different factors due to very limited and sparse vegetation. We differentiated between topsoil (the first 30 cm of mineral soil) and subsoil (> 30 cm) mineral layers as in recent reviews looking at the global distribution of soil organic matter fractions[11,16]. When multiple depths were sampled within each of our categories, we calculated the depth-weighted mean SOC, POC and MAOC at topsoil and subsoil depths. We finally gathered 37 studies representing 162 observations (Extended Data Fig. 1). See Appendix S1 for a list of the articles included in the meta-analysis. The full records of selected articles and the flowchart of preferred reporting items for systematic reviews and meta-analyses (PRISMA) can be found in Extended Data Fig. 6.

Mean, standard deviation and sample size of SOC, POC and MAOC were extracted directly from tables or from graphs using WebPlotDigitizer (https://automeris.io/WebPlotDigitizer/). We focused on physical soil organic matter fractionation[10,46], and included both particle size (MAOC lower than 50–63 µm) and density (MAOC heavier than 1.6–1.85 g cm^{-3}) methods as in recent global analyses[11,16], because they give very similar results in comparison studies[47] and in their response to environmental variation[39]. The number of observations using the particle size, density and combined size-density were 87, 51, and 24, respectively. When POC and MAOC were split into different components in combined size-density fractionation methods, fractions were summed to total MAOC and POC[39], and using SOC concentration and the percentage of each fraction.

We gathered a set of methodological, climate and soil variables from papers and global databases to explore their potential relationships with SOC, POC and MAOC: latitude (-54.26 to 78.73), longitude (-156.61 to 177.40), MAT (-18.6 to 3.9ºC), MAP (76 to 1,520 mm), biome (arctic, subarctic, alpine), soil depth (0 to 126 cm), soil pH (3.29 to 9.10), and soil clay + silt content (3.2 to 97.7%). When multiple depths were sampled, we calculated the depth-weighted mean soil properties at surface and subsoil depths. The biome of each site was categorized as arctic, subarctic or alpine following the Köppen-Geiger climate classification. Basically, the average warmest air temperature of any month is below 10ºC at arctic sites, one to three months average above 10ºC at subarctic sites, and one to five months average above 10ºC at alpine sites of the Qinghai-Tibet Plateau. We checked the warmest temperature of any month of the 1900-2019 period using CRUTEM4 accessed through Google Earth[48]. We obtained the mean annual temperature and precipitation of each field study site from the WorldClim v2.1 database[49], which provides average climatic values for the period 1970–2000. We used the NDVI from the MODIS satellite imagery MOD13Q1 product as our proxy of net primary productivity (NPP), as multiple studies have suggested the existence of a positive relationship between NDVI derived from AVHRR/NOAA satellite data and either biomass or annual aboveground net primary production (ANPP) for different geographic areas and ecosystems[50]. We followed the standard procedure for NDVI calculation at a global scale[51]. We acquired 23 NDVI values per year with a pixel size of 250 × 250 m and used them to calculate annual NDVI data for each year in the period from 2000 to 2021. To do so, we averaged the product values between the date of the minimum NDVI (*n*) and the date *n* – 1 of the following year at each site. MODIS data are geometrically and atmospherically corrected, and include a reliability index of data quality based on the environmental conditions in which the data were recorded and ranging from 0 –good quality data– to 4 –raw or absent data. When pixel reliability values were higher than 1, and to avoid using poor quality data such as pixels covered by snow, NDVI data were discarded.

When not reported in papers, we extracted soil pH and sand content from SoilGrid 2.0 (https://soilgrids.org/). We also specified whether the site has active permafrost soil or not. If yes, we recorded the thickness of the active layer (in cm) to assess as a surrogate of warming-induced permafrost thaw[27,28]. Gaps in data on the active layer of permafrost sites were filled with either published papers from the same site or using data from the Permafrost Climate Change Initiative[52].

Meta-analysis of experimental warming effects on soil carbon fractions in cold systems vs. other biomes

We synthesized studies that evaluated the effects of climate warming on SOC, POC and MAOC concentrations (g C kg soil^{-1}) in the mineral layer using pairwise field comparisons located side by side under the same climatic and soil conditions. A literature search was conducted on 4th May 2022 in the ISI Web of Knowledge with no restriction on publication year using the following term combinations: (soil carbon) and (fraction* or POM or MAOM or mineral or particulate or physical protection or light fraction* or macroaggreg* or microaggreg* or occluded or stabiliz* or persisten*) and (warming or elevated temperature*). We screened published reviews to check completeness of our literature compilation[39]. Then, we confronted this list with our selection criteria (see Supplementary Table 2). Data from one unpublished study performed at the CiPERH site in Alaska[45] meeting the selection criteria were also included in the database. We finally gathered 20 articles representing 40 observations. See Appendix S2 for a list of the articles included in the meta-analysis. The full records of selected articles and the flowchart of PRISMA can be found in Extended Data Fig. 7.

Mean, standard deviation and sample size of SOC, POC and MAOC at control (ambient temperature) and warming (elevated temperature) plots were extracted directly from tables or from graphs using WebPlotDigitizer (https://automeris.io/WebPlotDigitizer/). The number of observations using the particle size, density and combined size-density were 8, 15, and 15, respectively. Climate warming treatments included open top chambers, infrared heaters, heating cables, geothermal, and altitudinal transplants. The biome of each site was categorized as cold system (arctic, subarctic and alpine) or other (rest of biomes) following the Köppen-Geiger climate classification. We focused our analyses on the first 30 cm of mineral soil, as the number of studies including subsoil (> 30 cm) measurements was very low. When multiple surface depths were sampled, we calculated the depth-weighted mean SOC, POC and MAOC. Besides biome we did not explore any other biotic, abiotic or methodological variables, as these have been comprehensively tested in ref[39] and are not necessary to address our very specific research question (i.e., does POC respond more strongly to warming in cold systems compared to other biomes?) given the "pairing" of control and treatment plots across potential confounding variables.

Data analyses

The POC and MAOC concentrations in the top mineral layer (the first 30 cm of mineral soil) and subsoil (> 30 cm) layers, and in the topsoil mineral layer of permafrost and non-permafrost soils, and in arctic, subarctic, and alpine biomes did not exhibit normal distributions (Fig. 1). For this reason, POC and MAOC concentrations were first compared using non-parametric paired Wilcoxon signed-rank tests. Then, we used parametric linear mixed-effects modelling on natural-log transformed C concentrations to provide support for the Wilcoxon tests and to control for the effects of climate, net primary productivity and soil properties, as well as to account for the lack of independence between observations. In particular, we built a model with a fixed effects term that included C fraction as a binary variable (POC or MAOC, 1 or 0), together with its interaction with soil depth (topsoil vs. subsoil), permafrost (permafrost vs. non-permafrost), and biome type (arctic, subarctic, and alpine), as well as MAT, MAP, NPP, soil pH, and clay + silt content as covariates. In the random term of the model, we used an intercept structure with study plot nested within study to account for the dependence between observations of different depths within the same plot and within the same study.

We also used linear mixed-effects modelling to compare the relative effect sizes of the potential environmental drivers (MAT, MAP, NPP, soil pH, and soil clay + silt content) on the concentration of each C fraction (POC and MAOC) in the first 30 cm of mineral soil. Spatial associations between observations within the same plot and within the same study were accounted for by random intercept structures in the mixed-effects models. For linear mixed-effects modelling, all numeric variables were standardized by subtracting the mean and dividing by two standard deviations, and binary variables rescaled to -0.5 and 0.5[53]. The coefficients and 95% confidence intervals of the models were computed by the restricted maximum likelihood method and bootstrapping (1000 simulations), and P-values were estimated based on Satterthwaite approximation. Variance inflation factors (VIFs) and generalized VIFs were calculated to check that the degree of multicollinearity was low (VIF < 2 and GVIF < 2.2 for all predictors).

To build confidence in our analysis of the potential environmental controls on POC and MAOC concentrations in the first 30 cm of mineral soil, we also ran random forest modelling. These models are based on the construction of regression trees on bootstrap samples (resampling data allowing for replacement) grown with a subset of predictors. The excluded 'out-of-bag samples are then used to calculate an unbiased error rate which is essentially a cross-validated error estimate, and thus, eliminates the need for an aside test set[54,55]. Random forests measure relative importance as to how much each predictor contributes to increasing model accuracy[54], here computed as the difference in mean square error (MSE) when a variable is held 'out-of-bag'. Variance explained (R^2) was calculated by dividing MSE by the variance of the original observations and then subtracting this from one[56]. Even though both analyses query data for different purposes (i.e., mixed effects models estimate effect sizes, whereas random forests explain variation in the outcome), we reasoned that confidence in our analysis of this compiled observational dataset would increase if two contrasting approaches led to similar conclusions.

Wilcoxon signed-rank tests, linear mixed-effects modelling and random forest analyses were carried out using R version 4.1.1[57] and the car[58], lme4[59], lmerTest[60], partR2[61] and randomForest v.4.7-1.1[56] packages.

We explored whether anthropogenic experimental warming affected SOC, MAOC and POC concentrations compared to control plots in cold regions and in other biomes using the log response ratio (RR) as the measure of effect size. The RR is a unit free index, which ranges from $-\infty$ to $+\infty$ and estimates the size of the impact and its direction. The RR is calculated as $\ln(X_W) - \ln(X_C)$, where X_W and X_C are the SOC, MAOC or POC in the warming and control plots, respectively. Zero RR values mean no difference between warming and control plots, and positive and negative values indicate higher and lower SOC, MAOC and POC in warming than in control plots, respectively. For the sake of data interpretation, the RR was converted into the mean percentage of change, being estimated as $(e^{RR} - 1) \times 100\%$.

To test whether RR significantly differed from zero, we assessed whether its 95% confidence interval (CI) overlapped zero using the open-source software OpenMEE[62]. Specifically, we tested whether the 'biome type' of the study (cold systems including arctic, subarctic and alpine vs. other biomes) influenced the effect sizes using weighted random-effects models and a restricted maximum likelihood estimation method. As several studies contributed more than one RR when multiple sites were considered, the variable 'study' was included as a random factor in the mixed-effect model. We explored the moderating effect of the categorical covariate 'biome type' on the RR using a meta-regression and an omnibus test[62]. The publication bias was assessed with Spearman's rank correlation tests to analyze the relationships between the effect size and the variance and sample size across studies. The effect sizes of SOC, MAOC and POC were not correlated with data variances or sample sizes ($P > 0.05$ in all cases).

Methods references

43. Tamocai, C. *et al.* Soil organic carbon pools in the northern circumpolar permafrost region. *Global Biogeochem. Cycles* **23**, 1–11 (2009).

44. Strauss, J. *et al.* Deep Yedoma permafrost: A synthesis of depositional characteristics and carbon vulnerability. *Earth-Science Rev.* **172**, 75–86 (2017).

45. Plaza, C. *et al.* Direct observation of permafrost degradation and rapid soil carbon loss in tundra. *Nat. Geosci.* **12**, 627–631 (2019).

46. Golchin, A; Oades, J M; Skjemstad, J. 0 & Clarke, P. Soil structure and carbon cycling. *Aust. J. Soil Res* **32**, 1043–68 (1994).

47. Poeplau, C. *et al.* Isolating organic carbon fractions with varying turnover rates in temperate agricultural soils – A comprehensive method comparison. *Soil Biol. Biochem.* **125**, 10–26 (2018).

48. Harris, I., Osborn, T. J., Jones, P. & Lister, D. Version 4 of the CRU TS monthly high-resolution gridded multivariate climate dataset. *Sci. Data* **7**, 1–18 (2020).

49. Fick, S. E. & Hijmans, R. J. WorldClim 2: new 1-km spatial resolution climate surfaces for global land areas. *Int. J. Climatol.* **37**, 4302–4315 (2017).

50. Bastos, A., Running, S. W., Gouveia, C. & Trigo, R. M. The global NPP dependence on ENSO: La Niña and the extraordinary year of 2011. *J. Geophys. Res. Biogeosciences* **118**, 1247–1255 (2013).

51. Justice, C. *et al.* An overview of MODIS Land data processing and product status. *Remote Sens Environ* **83**, 3-15 (2002).

52. Obu, J. *et al.* ESA Permafrost Climate Change Initiative (Permafrost_cci): Permafrost version 2 data products. Centre for Environmental Data Analysis. http://catalogue.ceda.ac.uk/uuid/1f88068e86304b0fbd34456115b6606f (2022).

53. Gelman, A. Scaling regression inputs by dividing by two standard deviations. *Stat. Med.* **27**, 2865–2873 (2008).

54. Cutler, D. R. *et al.* Random forests for classification in ecology. *Ecology* **88**, 2783–2792 (2007).

55. Breiman, L. Random forests. *Mach Learn* **45**, 5–32 (2001)

56. Liaw, A. & Wiener, M. Classification and regression by randomForest. *R news* **2**, 18–22 (2002)

57. Team, R. C. R: A language and environment for statistical computing. (2021).

58. Fox, S; Weisberg, J. An R Companion to Applied Regression. Third edition. Sage, Thousand Oaks CA (2019).

59. Bates, D., Mächler, M., Bolker, B. M. & Walker, S. C. Fitting linear mixed-effects models using lme4. J. Stat. Softw. 67, (2015).

60. Kuznetsova, A., Brockhoff, P. B. & Christensen, R. H. B. lmerTest Package: Tests in Linear Mixed Effects Models. J. Stat. Softw. 82, 1–26 (2017).

61. Stoffel, M. A., Nakagawa, S. & Schielzeth, H. partR2: Partitioning R2 in generalized linear mixed models. bioRxiv (2020).

62. Wallace, B.C. *et al.* OpenMEE: Intuitive, open-source software for meta-analysis in ecology and evolutionary biology. *Methods Ecol. Evol.* **8**, 941–947 (2016).

63. García-Palacios, P. & Plaza, C. Dominance of the particulate organic fraction of

soil carbon in the top mineral layer of cold regions. *Figshare* https://figshare.com/s/7f1207628b0dda47d235 (2023).

Corresponding author

Pablo García-Palacios. E-mail: pablo.garcia@ica.csic.es

Acknowledgements

We thank all authors who gathered and published the raw data in the original studies that enabled this literature synthesis. P.G.-P. acknowledges support from the Spanish Ministry of Science and Innovation via the I+D+i project PID2020-113021RA-I00 and the TED project TED2021-130908A-C42 (funded by European Union - NextGenerationEU). Work at Lawrence Livermore National Laboratory by N.W.S. was performed under the auspices of the U.S. DOE OBER, under contract DE-AC52-07NA27344 award #SCW1632. M. Panettieri acknowledges financial support by the Comunidad de Madrid and the Spanish National Council of Scientific Researches research grant Atracción de Talento (grant number 2019T1/AMB14503).

Author Contributions

P.G.-P., M.A.B. and C.P. designed the research. P.G.-P., I.B.-F., J.C.G.-G., A.G., M.P., A.R., & C.P. conducted the literature synthesis. P.G.-P., M.d.C., J.J.G. & C.P. conducted the data analyses. The paper was drafted by P.G.P., and all authors contributed to the final version.

Competing interests:

Authors declare that they have no competing interests.

Data and materials availability:

All data will be made publicly available in a public repository (Figshare) upon publication and is temporarily available for manuscript review in the following link (https://figshare.com/s/7f1207628b0dda47d235)[63].

Extended data figures

Extended Data Figs. 1 to 7.

Supplementary Information

Appendix S1 and S2.

Supplementary Tables S1 and S2.

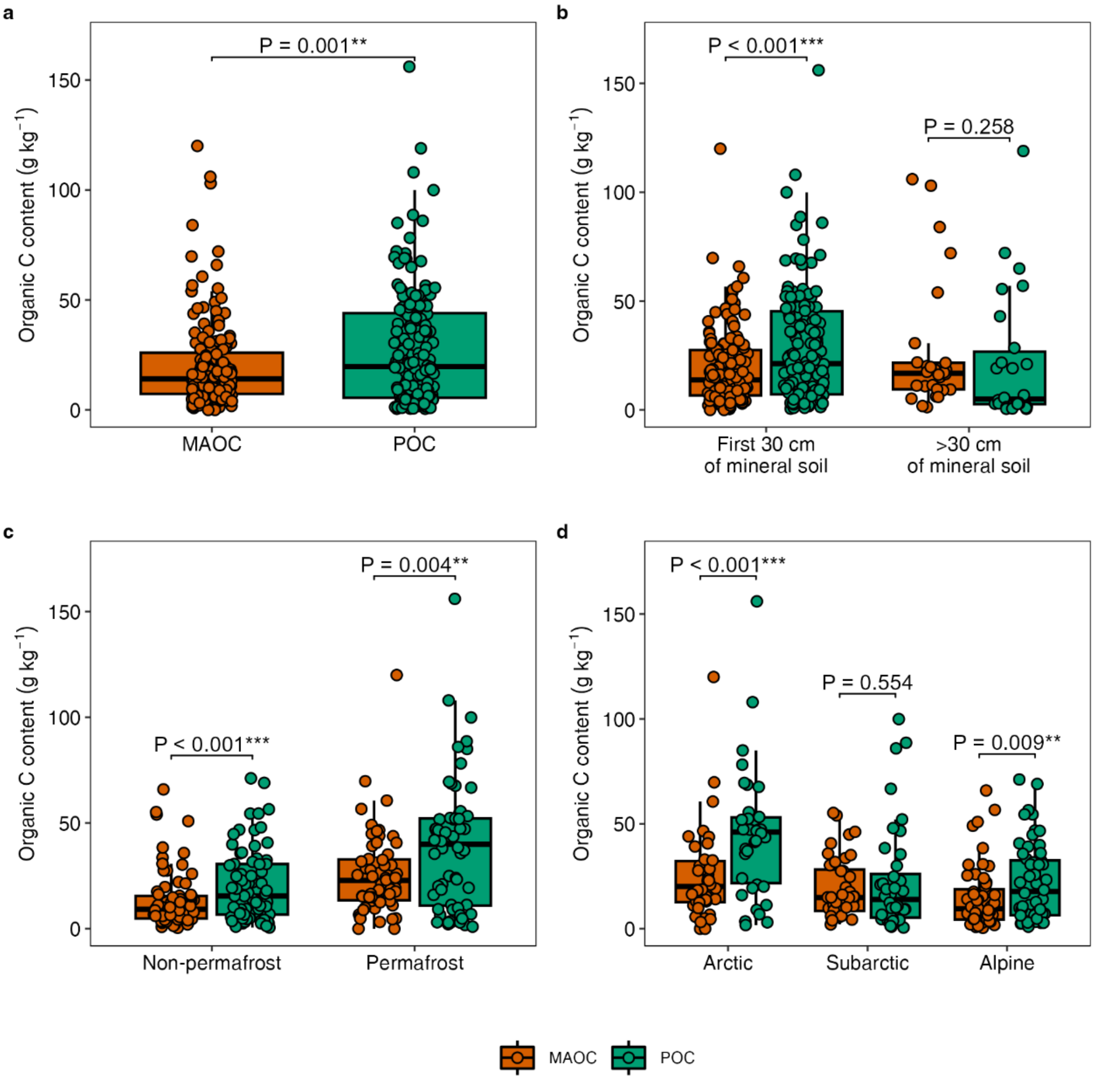

Figure 1 | Distribution of soil organic carbon in the POC and MAOC fractions (g C kg soil^{-1}) in the mineral layer of cold regions. Panels represent (a) overall fraction distribution or separated by (b) soil depth (the first 30 cm of mineral soil and >30 cm), (c) permafrost vs. non-permafrost soils, and (d) biome type. Results from paired Wilcoxon signed-rank tests. POC = particulate organic C; MAOC = mineral-associated organic C. Data in panels (c) and (d) correspond to the first 30 cm of mineral soil. Box plots represent 1st and 3rd quartiles (box), medians (central horizontal line), largest value smaller than 1.5 times the interquartile range (upper vertical line), and smallest value larger than 1.5 times the interquartile range (lower vertical line).

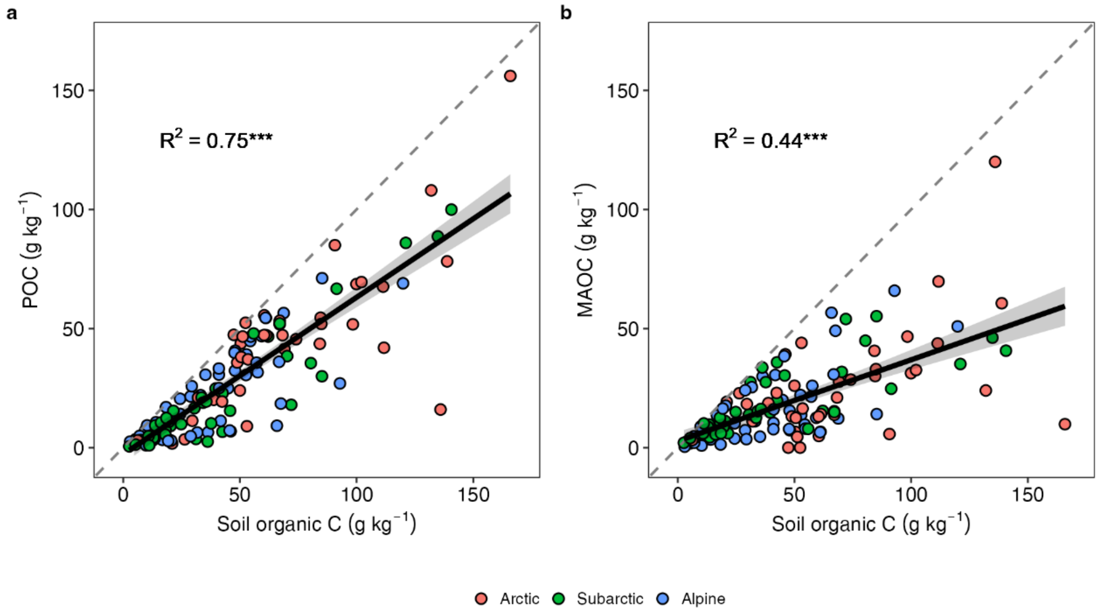

Figure 2 | Relationships between soil organic carbon and (a) POC and (b) MAOC concentrations in the top mineral layer of cold regions. Lines and shadings represent linear regression and 95% confidence intervals. MAOC = mineral-associated organic C; POC = particulate organic C. All panels correspond to the first 30 cm of mineral soil. *** $P < 0.001$.

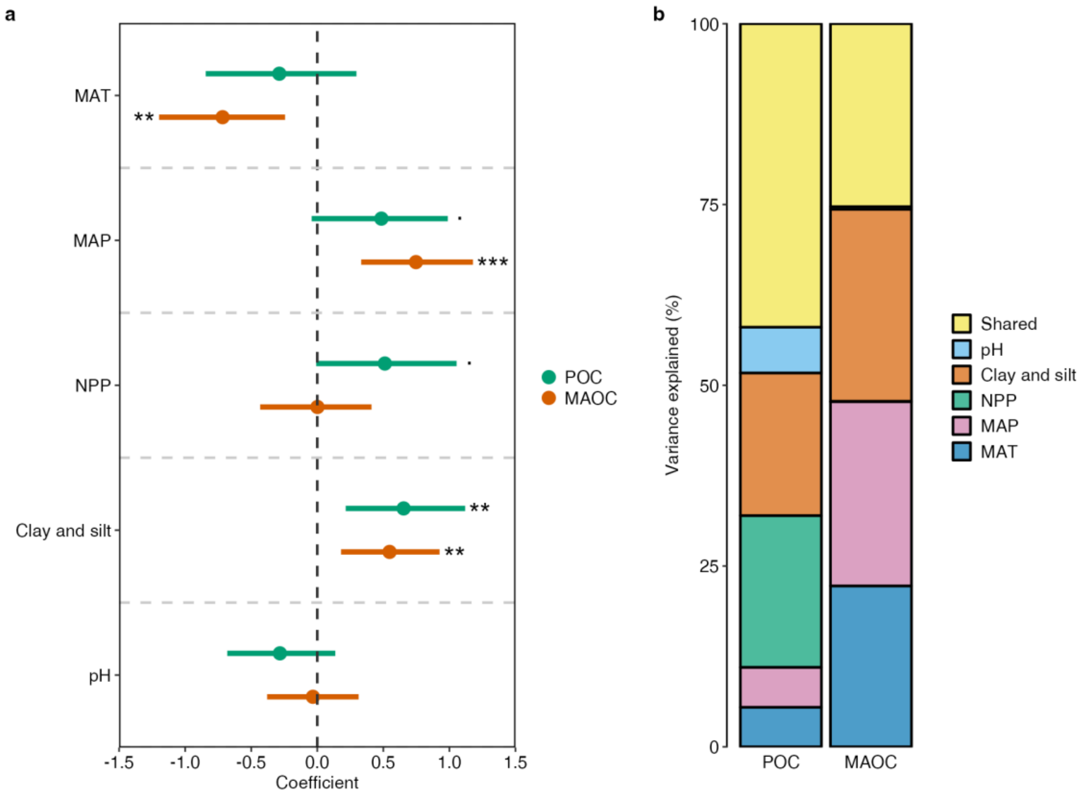

Figure 3 | Effects of environmental drivers on POC and MAOC concentrations in the top mineral layer (first 30 cm) of cold regions. Panels represent (a) coefficients (dot) and 95% confidence intervals (lines) of the fixed effects of mean annual temperature (MAT), mean annual precipitation (MAP), net primary productivity (NPP), soil pH, and soil clay + silt content in a linear mixed effects model (· $P < 0.1$, ** $P < 0.01$, *** $P < 0.001$), and (b) percentage of the variance explained by the fixed effects uniquely attributable to each predictor and shared among them. The variance explained by the fixed effect predictors and random effects relative to the total variance (R^2) was 30% and 36%, respectively, for POC, and 29% and 14% for MAOC. POC and MAOC concentrations were natural log-transformed. MAOC = mineral-associated organic C; POC = particulate organic C.

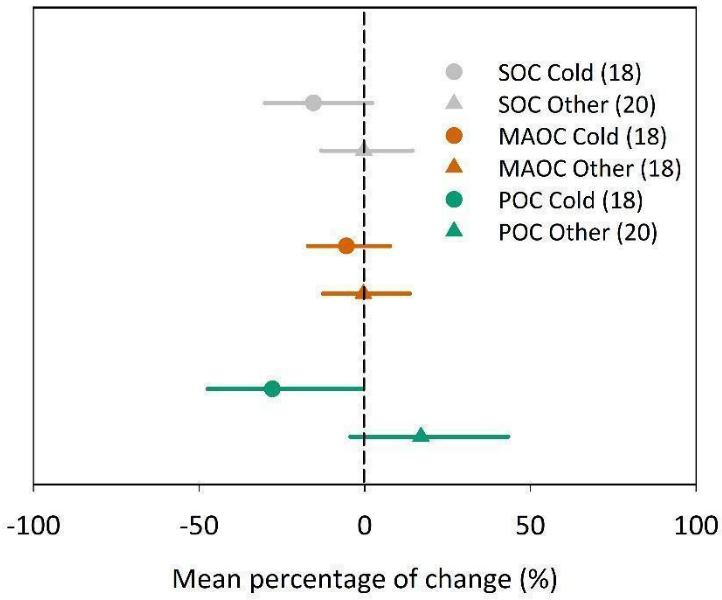

Figure 4 | Mean effect size of experimental warming on SOC, POC and MAOC in the top mineral layer (first 30 cm) of cold systems vs. other biomes. SOC = soil organic carbon; MAOC = mineral-associated organic C; POC = particulate organic C. Lines around symbols (log response ratios) are 95% confidence intervals.